Title
Novel Characteristics of VUV Insertion Device Beamlines at the Advanced Light Source (ALS)

Authors
Warwick, T.
Heimann, P.

Publication Date
1991-10-01

LBL-31533
UC-406

Lawrence Berkeley Laboratory
UNIVERSITY OF CALIFORNIA

Accelerator & Fusion Research Division

Presented at the Seventh National Conference on Synchrotron Radiation Instrumentation, Baton Rouge, LA, October 28–31, 1991, and to be published in the Proceedings

Novel Characteristics of VUV Insertion Device Beamlines at the Advanced Light Source

T. Warwick and P. Heimann

October 1991

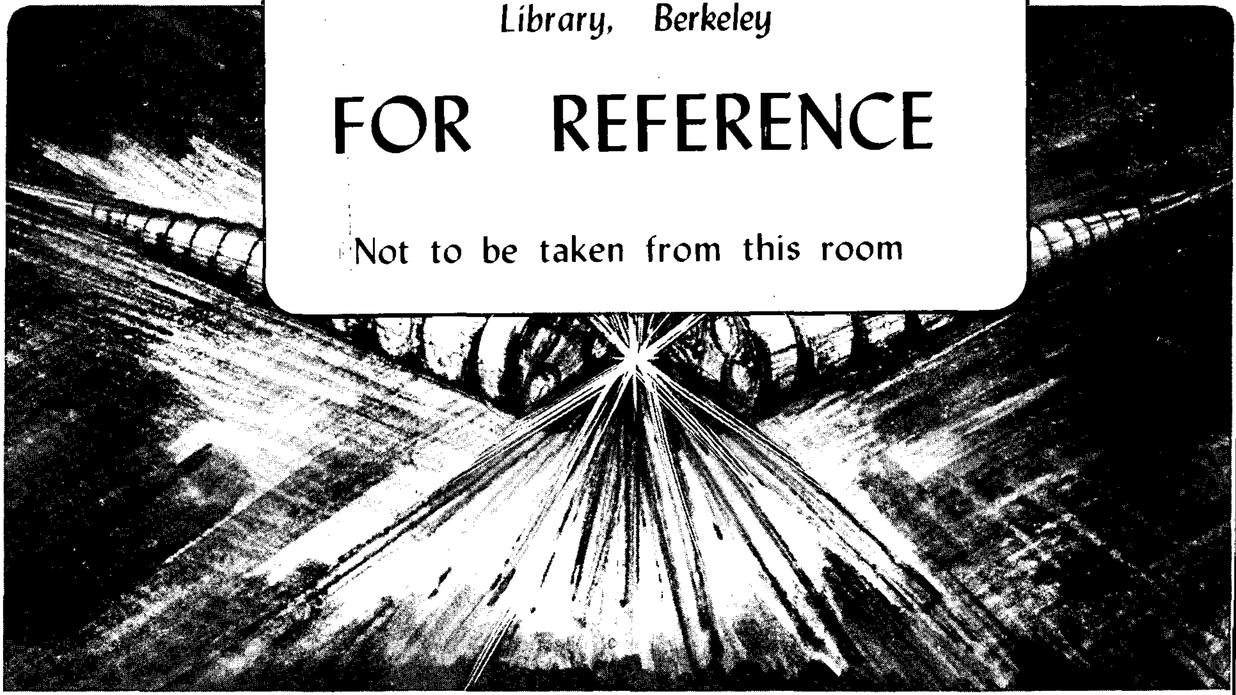

Prepared for the U.S. Department of Energy under Contract Number DE-AC03-76SF00098

LBL-31533

NOVEL CHARACTERISTICS OF VUV INSERTION DEVICE BEAMLINES AT THE ADVANCED LIGHT SOURCE*

T. Warwick and P. Heimann

Advanced Light Source
Accelerator and Fusion Research Division
Lawrence Berkeley Laboratory
University of California
Berkeley, CA 94720

October 28, 1991

Paper presented at the Synchrotron Radiation Instrumentation Conference, Baton Rouge, LA, October 28–31, 1991

*This work was supported by the Director, Office of Energy Research, Office of Basic Energy Sciences, Materials Sciences Division of the U.S. Department of Energy, under Contract No. DE-AC03-76SF00098

Novel Characteristics of VUV Insertion Device Beamlines at the Advanced Light Source

Tony Warwick and Philip Heimann

Lawrence Berkeley Laboratory,
Berkeley, CA 94720, USA.

The design of VUV beamlines for the Advanced Light Source is discussed. Features of the design serve to illustrate the careful attention required in order to preserve the performance of the low emittance 'third generation' storage ring, operating with insertion devices.

1. Introduction.

The Advanced Light Source is designed to operate with a horizontal emittance of 10^{-8} m rad or smaller with about 10% coupling into the vertical direction [1]. The corresponding r.m.s. beam size and divergence at the center of an insertion straight section are given in Table 1. Such a bright source of synchrotron radiation offers one or two orders of magnitude more flux of energy–resolved photons than are presently available from VUV beamlines at existing facilities.

In order to take advantage of this improved performance, a number of stringent conditions must be met.

a). The undulator magnetic field errors must be small.

b). The undulator gap must be tuned in cordination with the monochromator scan, so that the peak of the brightness curve is always at the selected wavelength.

c). The undulator beam must be precisely stable.

d). Beamlines and monochromators must be designed for maximum transmission efficiency.

e). Optics must be carefully cooled to avoid deformation of the reflecting surface.

Examples are given in the following sections showing how each of these problems is being tackled in the designs of the first two undulator beamlines at the ALS, which are known as U5 and U8, because they operate with radiation from a 5cm and an 8cm period undulator, respectively. Figure 1. shows a schematic diagram of the optical layout of these two beamlines, each of which includes a spherical grating monochromator with moving exit slits [2]. A condensing mirror images the source onto an entrance slit and refocus optics generate a small spot on the sample.

2. Undulator errors and undulator tuning.

Random and systematic field errors in insertion devices affect the spectral brightness. Since the first,third and fifth harmonics are all to be used to extend the operational energy range, and of these the fifth is most sensitive to errors, we use this harmonic to determine error limits.

Systematic variation of K along the length of the undulator will broaden the spectral peaks. This is tolerated up to about 50% broadening [3] and leads, in the U5.0 case, to a tolerance on the K variation of 0.18%, corresponding to a tolerance on the gap uniformity, when the undulator is closed, of about 60μm.

Random errors diminish the spectral peaks and re-distribute the energy throughout the spectrum [4]. The r.m.s. random error in the (vertical) magnetic field, for U5.0, must be less than 0.25% to keep the peak reduction of the fifth harmonic less than 30%.

Figure 2. shows a computed spectrum [5] from the 5cm period undulator with 89 periods, 4.5m long, without field errors but including the effects of the electron beam emittance. This is the spectrum transmitted by an aperture matching the diffraction limited size of the undulator central cone. It will be possible to operate the beamline with a larger aperture, but off-axis radiation will represent a less-bright source and spot sizes at the sample will be increased. It is apparent that, in order to exploit the brightness, the undulator must be precisely tuned, so that the required wavelength is delivered at the peak of the appropriate spectral harmonic. The flux shown for the fifth harmonic in figure 2. will be reduced to about half by the undulator errors that we tolerate, which will have much less effect on the intensity of the fundamental peak.

Large-aperture vacuum chambers will be installed in the straight sections during comissioning of the ALS. These chambers will limit the magnetic gap to 2.4 cm or larger, instead of the final design value of 1.4 cm. Figure 3. shows the brightness tuning curves under these circumstances. It is clear that the storage ring commissioning must proceed to the point where the smaller chambers can be installed in order to realize the full performance.

The temperature coefficient of the magnetization of Nd–Fe–B permanent magnets is about 10^{-3} °C^{-1} so that to limit the thermal shift of the spectrum to half the width of the fifth harmonic, the temperature of the undulator environment must be stable to ±1°C.

3. Stabilization of the undulator beams.

Whether the monochromators employ entrance slits or not, the position of the source of the undulator beam must be stable. Two photon position monitors with 2μm resolution [6] will be installed on stable pillars, 8m and 12m from the center of the straight section. Error signals will be processed digitally into a feedback loop to control the currents of four steering dipoles upstream and downstream of the insertion device, in an orbit bump localized to that section of the storage ring. This loop will stabilize thermal drifts, but its response will be limited to frequencies below about 10Hz by eddy currents in the thick aluminum vacuum chamber and it may be ineffective against mechanical and electrical oscillations, which will then have to be minimized at their source.

In the particular case of the first two undulator beamlines, the pitch of the condensing mirror must be adjustable with a resolution of about 0.1μrad, in order to steer the focussed beam through the entrance slit. A feedback loop is feasible here too, and tests with the first mirror show a frequency response up to 50 Hz with a DC loop gain of 10 or 20.

4. Monochromator transmission efficiency.

Figure 4. shows the transmission of various components of the U5 beamline. The condensing mirror is fixed. The entrance slit width is set to give a slit–width–limited resolving power of 10,000 and the computed slit transmission includes the effects of aberrations of the spherical mirror. Curves are shown for each of the three diffraction gratings in the U5 monochromator. The entrance slit width varies from about 20μm to about 5μm as the photon energy is increased. When the monochromator is actually operated for high resolution the slits will probably be fixed at 10μm, since aberrations and grating

slope errors will limit the resolving power to values of about10,000 or less. The slit transmission should typically be about 60%. The grating will have a ruled length of at least 14cm and will collect all the light except close to the horizon. The diffraction efficiency is calculated using a geometric model [7], and is multiplied by the grating reflectivity at the appropriate angle. This approximate treatment has been found to agree closely with complete electromagnetic calculations [8] for test cases.

Figure 5. shows the resolved flux from each of three gratings for the U5 beamline. The electron current is 400 mA and the gratings G1, G2 and G3, with ruling densities of 150, 330 and 720 lines/mm, use the first, third and fifth undulator harmonics respectively. Undulator errors are not included and will reduce the flux at high energies by as much as a factor of two.

Analysis of the transmission of the U8 beamline shows very similar results, delivering photons from 20eV to 300eV.

5. Thermal distortion of optics.

It is well understood that the condensing mirror in these beamlines must be cooled with internal water channels close to the reflecting surface, to keep thermal deformation of the surface figure to acceptable levels. These thermal effects must not affect the entrance slit transmission. The condensing mirror can absorb up to about 100W, at K=4 on the U5 beamline. Under this maximum heat load the geometrical aberrations of the mirror are also at their largest, and we ask that the r.m.s. tangential ray deviation due to thermal deformation be no more than 50% of the deviation of the r.m.s. ray due to the third order aberration. This tolerance is met in the mirror thermal design calculations and will render thermal effects negligible.

The specification for cooling the grating is less clear, with 60% entrance slit transmission it may absorb about 18W in the U5 monochromator. One could compromise by trading flux for resolution, and simplify the cooling scheme. We have chosen not to make this compromise, since water cooling of some kind is required and a design for internal channels is available. The tolerance for deformation is then derived in the following way. The thermal deformation is considered as a change in the grating radius over the heated region of the surface, which is a good approximation to the shape of the thermal surface deformation. The heating provides an 'added radius' ($R_{thermal}$) and the new radius is given by:

$$1 / R = 1 / R_{polished} + 1 / R_{thermal}$$

Figure 6. shows the tolerable added radius due to thermal effects, as the U5 monochromator is scanned over the energy range of one of the 3 gratings. This is the thermal deformation which gives a spread of wavelength at the exit slit equal to either a) the spread due to the third order geometrical aberration (coma) or b) the contribution from 10μm entrance slits, whichever is larger.

defocus:

$$\Delta\lambda = (2/Nk) \quad w \quad \{(\cos^2\alpha)/r-(\cos\alpha)/R+(\cos^2\beta)/r'-(\cos\beta)/R\}$$

coma:

$$\Delta\lambda = (3/2Nk) \quad w^2 \, \{[(\cos^2\alpha)/r-(\cos\alpha)/R](\sin\alpha)/r + [(\cos^2\beta)/r'-(\cos\beta)/R](\sin\beta)/r'\}$$

entrance slit:

$$\Delta\lambda = (1/Nk) \quad s \quad (\cos\alpha)/r$$

(N is the ruled density, k the diffracted order, α and β are the angles of the incoming and outgoing ray at the grating, w is the illuminated half–length, r and r' are the entrance and exit arm lengths, R is the grating radius and s is the full width of the entrance slit)
Thermal design calculations of the grating show the specification met, with an 'added radius' of 110km when 30W is absorbed. Details of the design of these optics can be found in reference [9].

6. Refocusing optics.

In each of these two beamlines a fixed horizontal mirror images the source at the sample. A vertical refocus mirror will be provided to collect the light diverging from the exit slit. The radius of this mirror will be adjustable, it will be a metal substrate bent into a circle [10]. By designing for unity magnification, geometrical aberrations are minimized. Engineering tolerances for the bender will be specified to give a spot with 50μm FWHM, which makes the bent substrate engineering feasible and, in the U5 case, matches the horizontal spot size. The inclusion of the refocus optics in the beamline design is very important to exploit the high flux of resolved photons for experiments such as photoelectron microscopy. The vertical mirror radius will be adjustable to focus the exit slit at any point within its range of travel. For the U5 beamline, the radius must change from 89m to 78m with a grazing angle of 2°. A limited scan of the monochromator is possible with constant mirror radius, until the defocus increases the spot size to more than 50μm, typically a scan of 5% in photon energy (up to 20% at the Rowland wavelength where the exit slit is moving slowly). Figure 7. illustrates the concept for the scan range covered by one of the gratings in the U5 monochromator.

7. Conclusions.

It seems challenging to take advantage of the high brightness offered by the 'third generation' synchrotron sources. At the ALS careful attention has been given to the design of two undulator beamlines as part of the initial complement of experimental systems. The design shows the possibility of delivering a flux of photons at high resolution about 2 orders of magnitude higher than presently available [11]. There remains the challenging task of implementing and commissioning these beamlines to achieve this goal.

This report represents the work of a two groups of people at the Advanced Light Source, known as the 'Beamline Engineering Group' under Dick DiGennaro and the 'Experimental Systems Group' under Brian Kincaid.

This work was supported by the Director, Office of Energy Research, Office of Basic Energy Sciences, Materials Sciences Division of the U.S. Department of Energy, under Contract No. DE-AC03-76SF00098

Table 1.

Nominal electon beam size and divergence at the center of an insertion device.

horizontal r.m.s. size σ_h	330 μm
horizontal r.m.s. divergence σ'_h	30 μ rad
vertical r.m.s. size σ_v	63 μm
vertical r.m.s. divergence σ'_v	16 μ rad

Figure Captions.

Figure 1. Schematic diagram of the optical arrangement of the first two undulator beamlines to be built at the ALS. Each includes a spherical grating monochromator with moving exit slits. A condensing mirror produces a demagnified image of the source at the fixed monochromator entrance slit. Refocus optics collect the vertically divergent light from the exit slit.

Figure 2. A computed spectrum for the 5cm period undulator with 89 periods, including the effects of electron beam emittance. This calculation is for a K value of 2.5 and shows the spectral flux through a $2\sigma \times 2\sigma$ rectangular aperture, where σ is the r.m.s. size of the central cone of undulator radiation. The electron current is 1 Ampere at 1.5 GeV.

Figure 3. Tuning curves for the 5cm period undulator. The on–axis brightness of the first three odd harmonics is shown as the K value is varied. The dashed portion of the curve will not be accessible until storage ring comissioning is complete and the small gap vacuum chambers are installed.

Figure 4. Transmission factors for the U5 beamline. The entrance slit is always adjusted to give a slit width resolving power of 10,000. The grating parameters are chosen to span the range of photon energy from 80eV to 1000eV.

Figure 5. Computed resolved flux for the U5 beamline after the exit slit. The grating parameters are chosen to operate up to 1 keV in this example. The gratings G1,G2 and G3 use the first, third and fifth undulator harmonics respectively. Undulator errors are not included and may reduce the flux in the fifth harmonic by as much as half.

Figure 6. The tolerable 'added radius' due to thermal distortion of the grating which gives a contribution to the resolution equal to that from the third order aberration of the grating, or the 10μm entrance slit width, whichever is greater.

Figure 7. An example of an adaptive vertical refocus mirror design to collect the divergent light from the exit slit. The mirror radius will

be adjustable from 89m to 78m to keep the moving slit in focus. The lowest part of the figure shows the defocus which develops as the monochromator is scanned around the Rowland wavelength with moving slit and constant mirror radius.

References.

[1]. "An ALS Handbook" PUB-643Rev. 2, Lawrence Berkeley Laboratory, April 1989.

[2]. H.Hogrefe, M.R.Howells and E.Hoyer, SPIE 733(1987)274

[3]. "U5 Undulator Conceptual Design Report" PUB-5256, Lawrence Berkeley Laboratory, November 1989.

[4]. B.M.Kincaid, Nucl.Inst.Meth.Phys.Res., A291(1990)363
B.M.Kincaid, J.Opt.Soc.Am., B2(1985)1294

[5]. R.P.Walker, Rev.Sci.Instr., 60(1989)1816

[6]. T.Warwick, D.Shu, B.Rodricks and E.D.Johnson, to be published, Proc. 4th Intl. Conf. Synch. Radn. Instr., Chester, England, 15-19 July, 1991.

[7]. J.M.Bennet, PhD thesis, Univ. London, 1971

[8]. W.Jark and M.Nevier, Appl. Opt. 26(1987)943
H.Padmore, private communication.

[9]. T.Swain, LSME 322, Advanced Light Source Internal Note, Lawrence Berkeley Laboratory, 1990
D.DiGenarro and D.Yee, LSME 372, Advanced Light Source Internal Note,Lawrence Berkeley Laboratory, 1990

[10]. M.R. Howells, private communication.

[11]. K.J. Randall et. al., Synchrotron Radiation News, correspondents report, to be published.

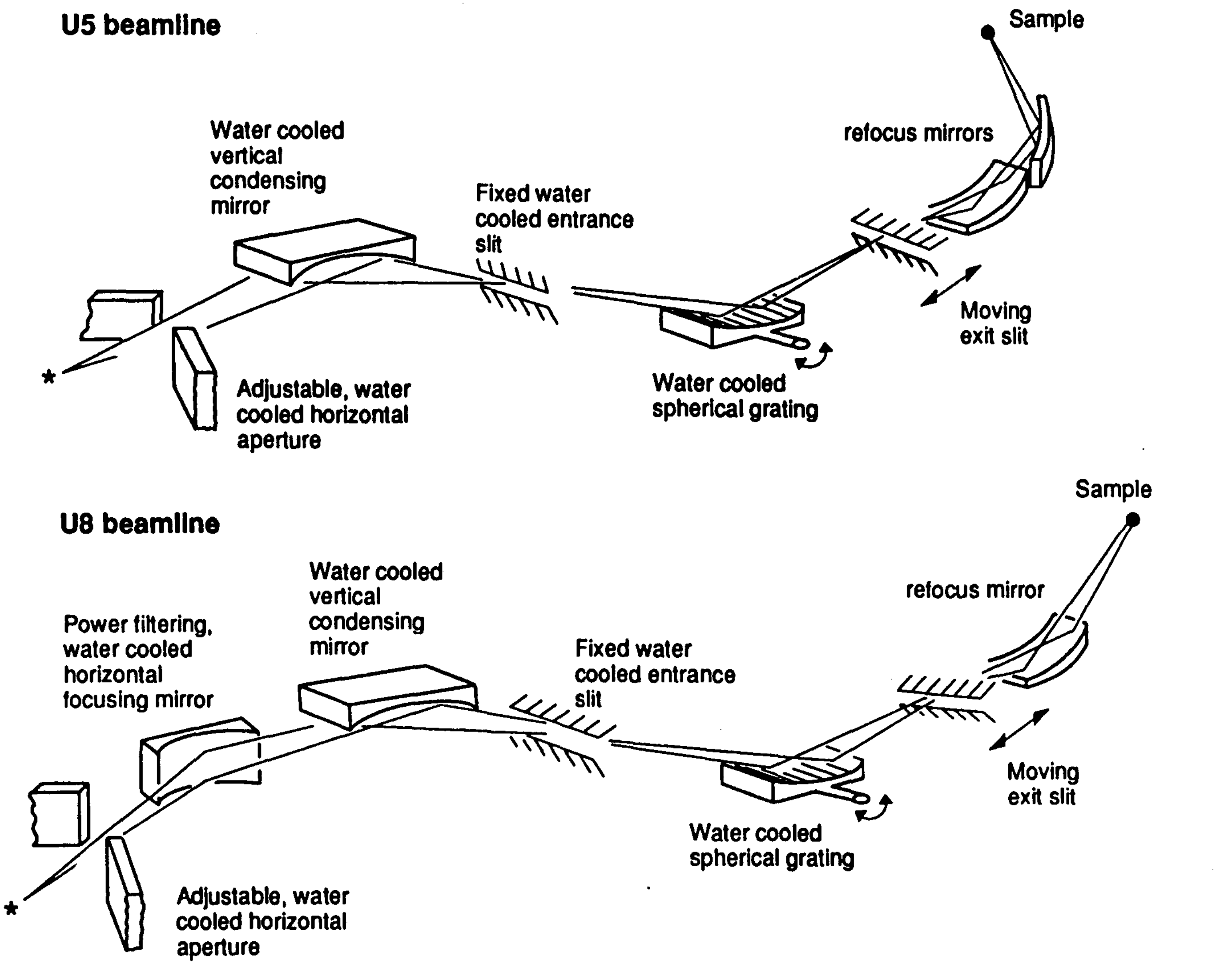

Figure 1

XBL 9111-6845

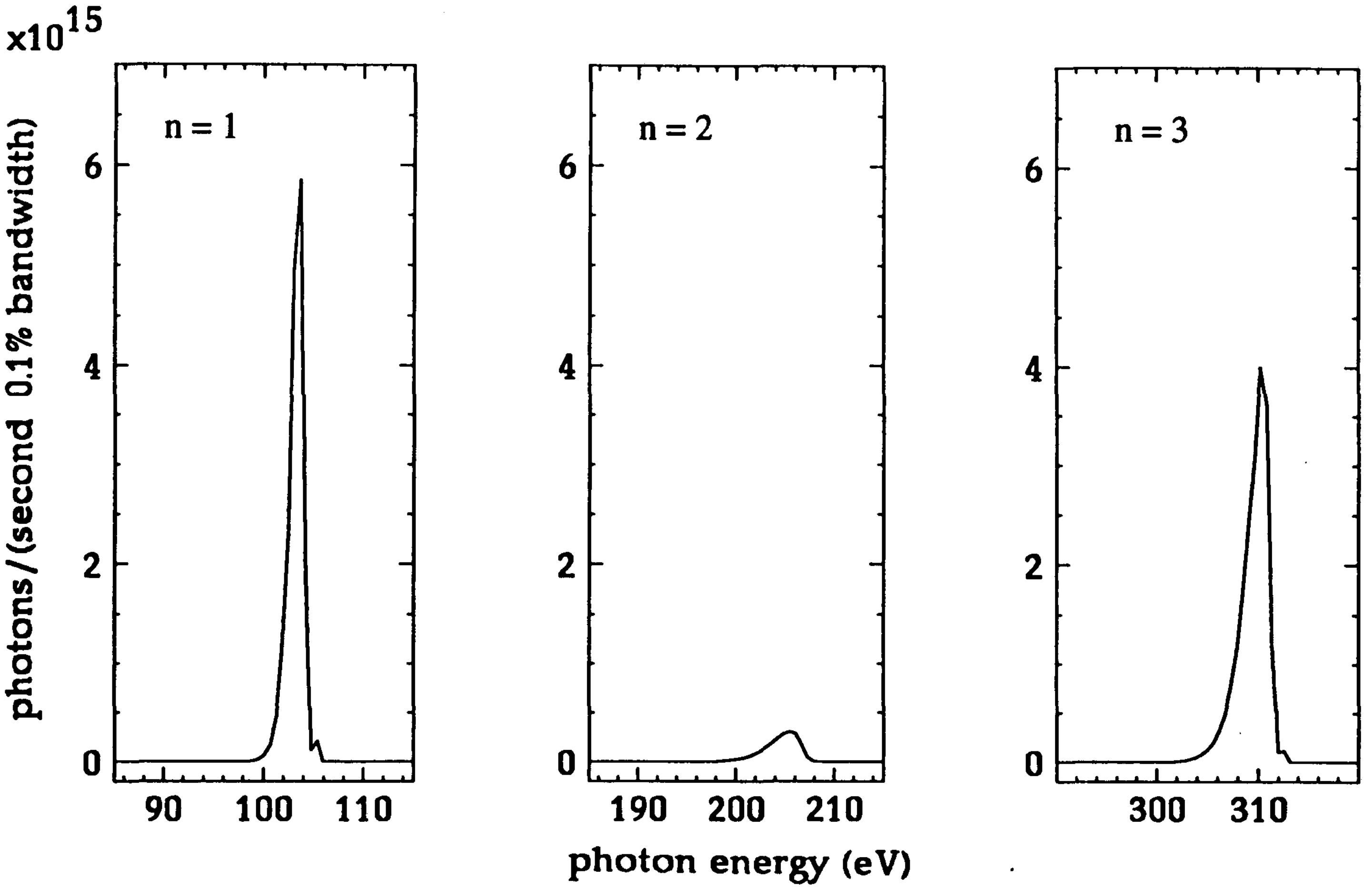

XBL 9111-6846

Figure 2

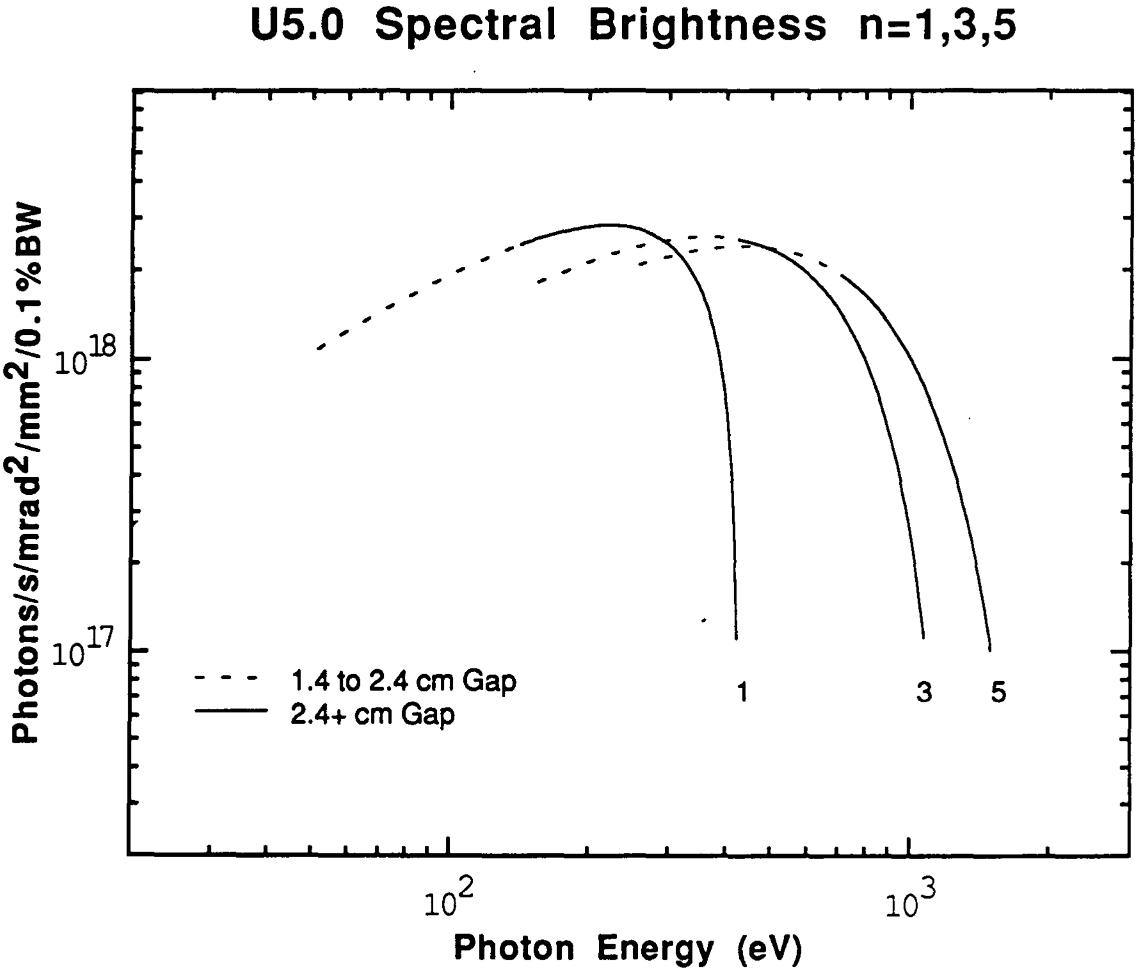

XBL 9111-6847

Figure 3

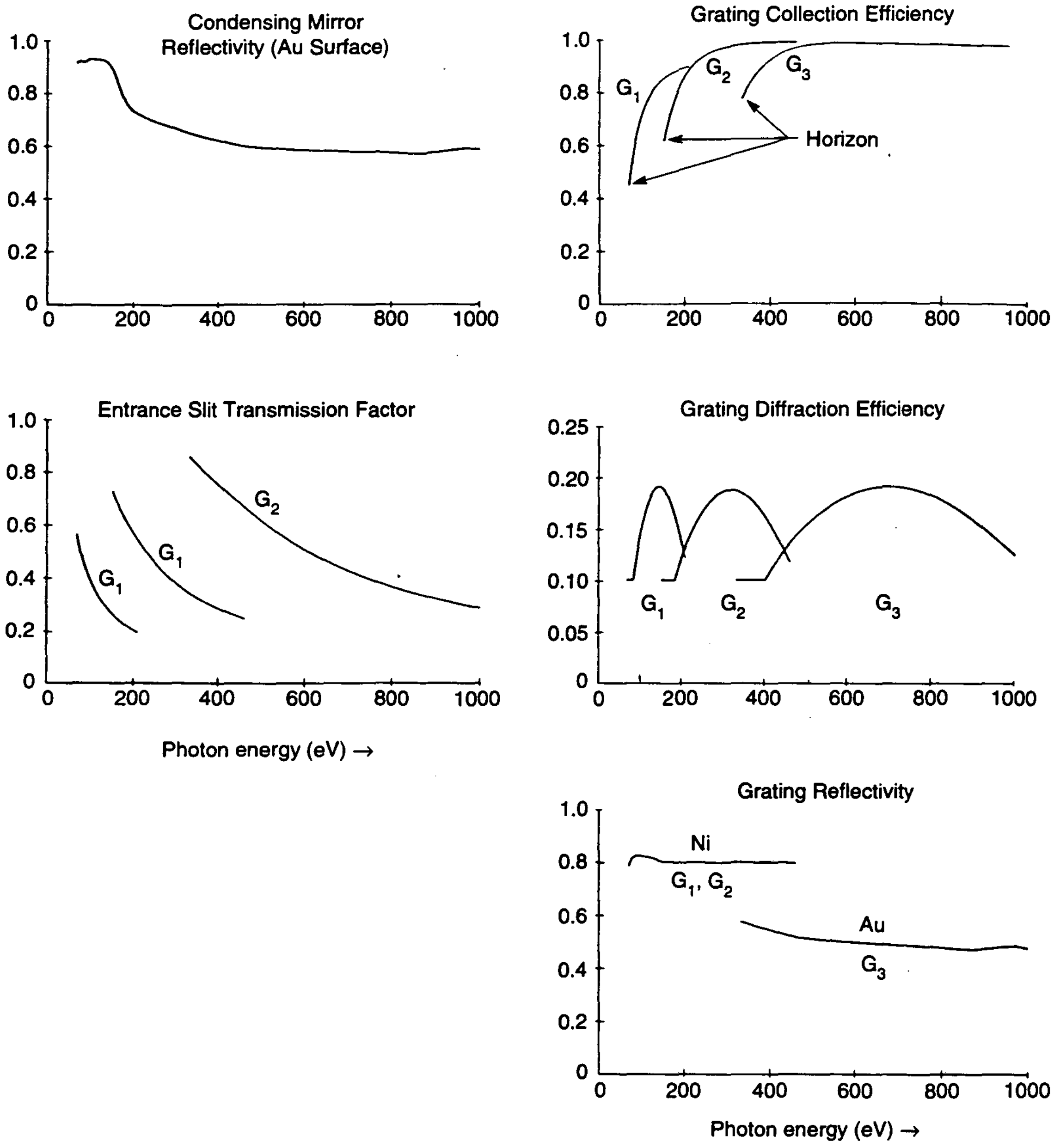
Condensing Mirror Reflectivity (Au Surface)

Grating Collection Efficiency

Entrance Slit Transmission Factor

Grating Diffraction Efficiency

Grating Reflectivity

XBL 911-6848

Figure 4

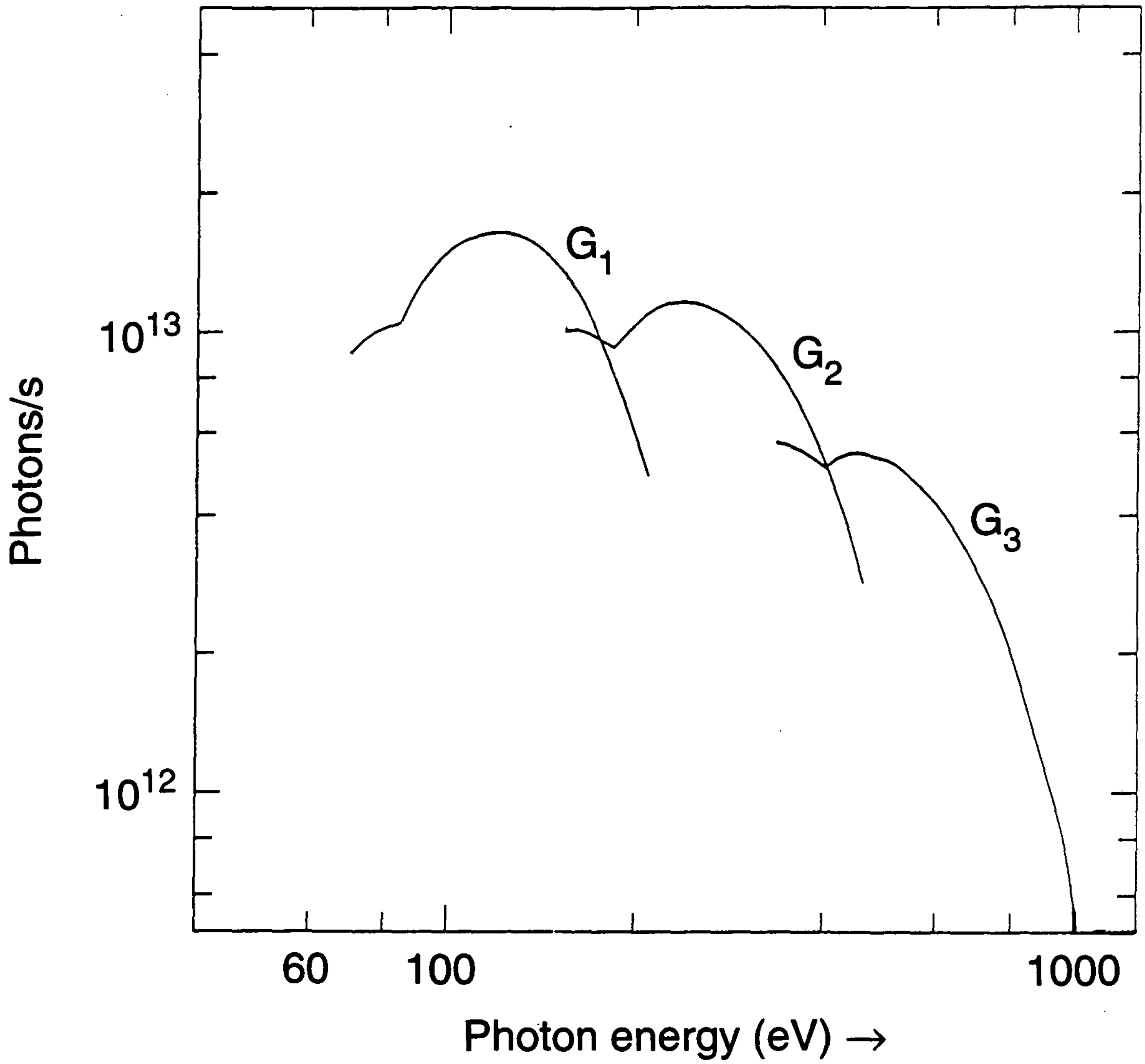

XBL 9111-6849

Figure 5

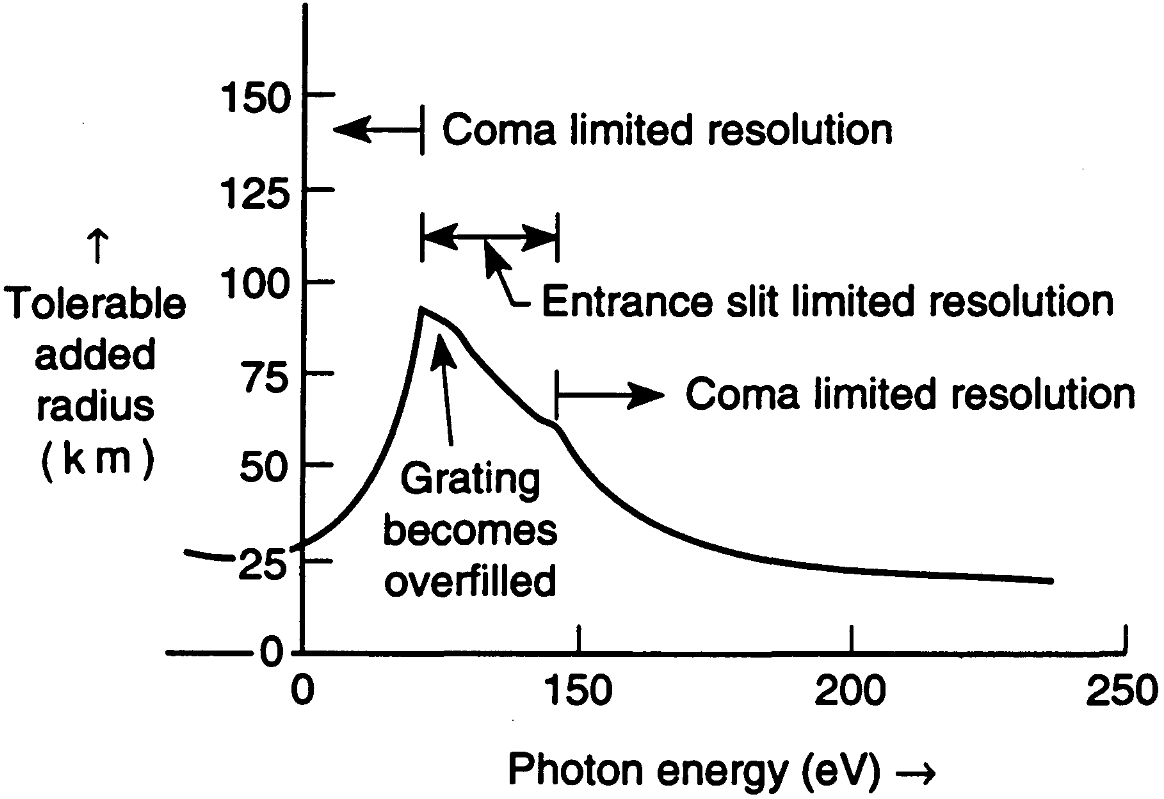

XBL 9111-6850

Figure 6

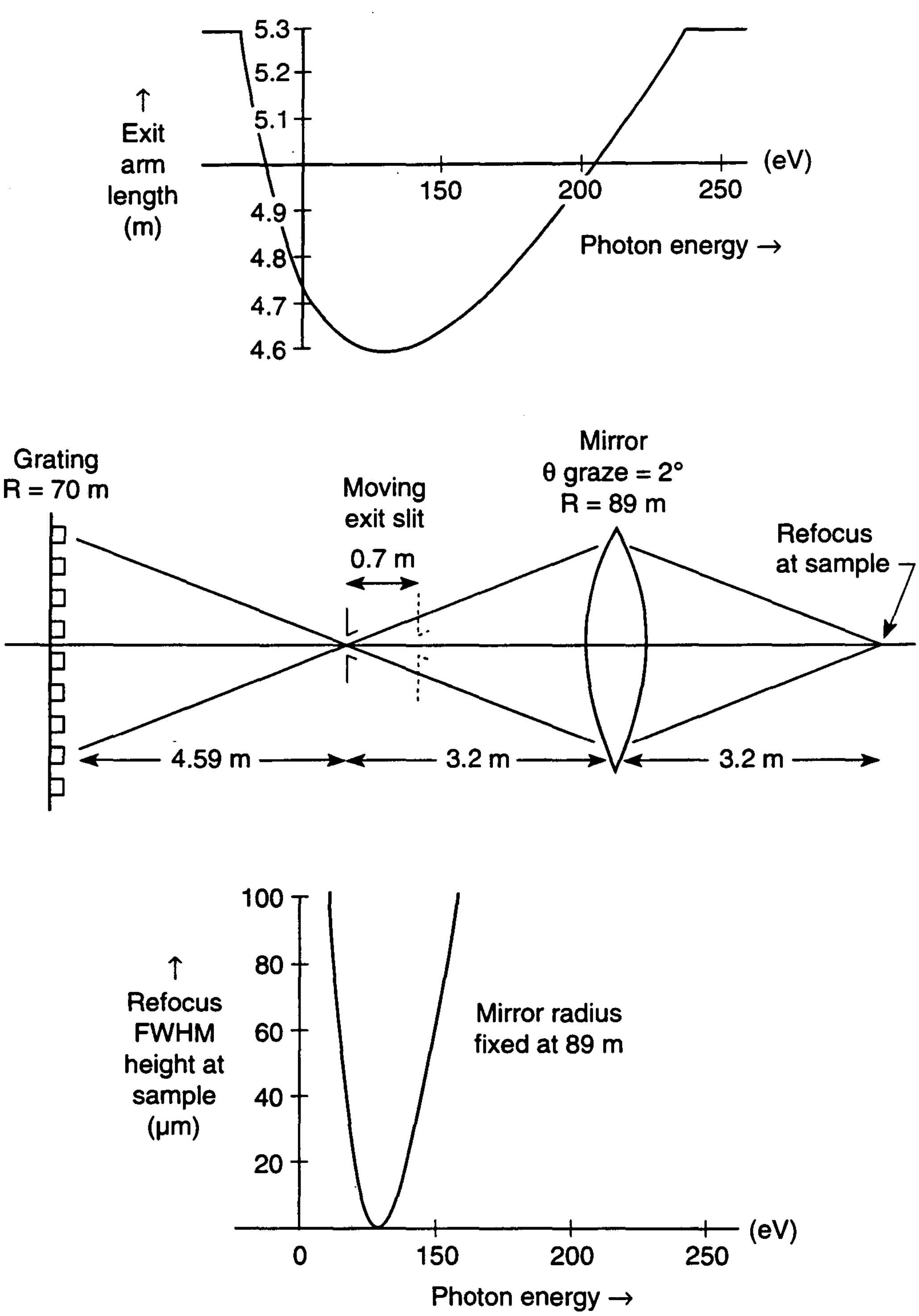

XBL 9111-6851

Figure 7

LAWRENCE BERKELEY LABORATORY
UNIVERSITY OF CALIFORNIA
TECHNICAL INFORMATION DEPARTMENT
BERKELEY, CALIFORNIA 94720